

INVESTIGATION OF THE REACTION MECHANISMS FOR PYROLYSIS OF
RUNDLE OIL SHALES BY DYNAMIC ^1H NMR TECHNIQUES

T. Parks, L.J. Lynch and D.S. Webster

CSIRO Division of Fossil Fuels, P.O. Box 136, North Ryde,
NSW, 2113, Australia

ABSTRACT

Dynamic proton nuclear magnetic resonance (^1H NMR) techniques were used to study the pyrolysis behaviour of a suite of Rundle oil shale ore types. Experimental results were obtained by monitoring the ^1H NMR transverse relaxation signal for both the shales and their kerogen concentrates during their pyrolysis by heating at a uniform rate in open glass tubes in an inert atmosphere provided by flowing nitrogen gas.

These results indicate that while the Rundle ore types have variable pyrolysis behaviour, all of the demineralized shales pyrolyse similarly. The differences observed in the behaviour of the shales are thought to be a consequence of variations in the permeability of the inorganic matrices to evolving volatile species. Enhancement of molecular mobility marks two transitions of the specimen during pyrolysis. The first, which occurs between room temperature and ~ 500 K and involves most of the structure, is probably a "glass to rubber" type transition and the second, which occurs near 600 K indicates the presence of a relatively thermally stable component in the kerogen. The results show that the pyrolysis residue formed above 750 K is contributed to by material that passes through a transient mobile state.

INTRODUCTION

Studies over many years of the pyrolytic decomposition of oil shales have led to a variety of kinetic models which invoke intermediate species referred to as pyrobitumens (1-3) and sometimes also as rubberoid (4) and polyoil (5) species. These intermediate species are at best only loosely defined and while it is expected that such intermediate states do occur during pyrolysis their delineation in composition and occurrence are still matters for investigation. In these models the original kerogen is usually treated as being homogeneous but recently kerogen pyrolysis has been analysed in terms of the chemically distinct aromatic and aliphatic fractions (6-8).

Dynamic measurement techniques have an advantage over equilibrium measurement techniques in such investigations because of their potential to monitor transient states of the reacting system. The adaptation of proton nuclear magnetic resonance (^1H NMR) as a dynamic measurement technique has been described previously (9-11). The hydrogen specificity of the ^1H NMR experiment aids in the distinction of thermal processes associated with the organic kerogen from those of the inorganic matrix of the shale. For organic solids the most important factors governing their ^1H NMR behaviour are the concentration and distribution of protons and unpaired electrons in the structure and the molecular dynamics. To this extent uncoupled or "broadline" NMR can provide information on the complex interactions which determine the molecular properties and form of the bulk material. These NMR measurements will detect molecular mobility changes associated with melting and other "softening" transitions and likewise transitions of the molecular lattice back to the rigid lattice state, the loss of hydrogen from the specimen during decomposition and changes in free radical concentrations related to bond rupture and condensation reactions. The results reported here are all derived from dynamic measurements of the ^1H NMR transverse relaxation signal $I(t)$. Parameters are derived from these measured signals which (a) represent the residual specimen as consisting of two

components, one containing rigid hydrogen and the other mobile hydrogen, (b) characterize the molecular mobility of the structure containing the mobile hydrogen, (c) estimate the residual hydrogen content and (d) characterize the ^1H NMR transverse relaxation signal $I(t)$ and therefore the total residue in terms of its average molecular mobility. The temperature dependences of these parameters form a set of pyrograms reflecting changes in the specimen during the pyrolysis.

EXPERIMENTAL

The shales studied were a suite of the ore types distinguished and characterized in the Rundle deposit by Coshell (12). Specimens in the form of -100 mesh powders were supplied by ESSO Australia together with chemical analysis and Fischer assay oil yield data (Table I). A composite Rundle shale has been reported as having a ^{13}C CP-MAS aromaticity value of about 0.22 (13). Kerogen concentrates were prepared by HCl/HF digestion of the mineral matter and subsequent analysis showed them to contain large quantities of fluorine and to have total ash contents in the range 17 to 38% (13).

Predried shale and kerogen concentrate specimens of ~ 400 mg contained in 8 mm O.D. open glass tubes were used for the ^1H NMR thermal analysis experiments which were conducted under nitrogen gas flowing at 5 ml min^{-1} . Comparative studies of the shale ore types and their kerogen concentrates were made in a series of pyrolysis experiments at a uniform heating rate of 4 K min^{-1} . The ^1H NMR measurements were made using the two pulse ($90^\circ\text{-}\tau\text{-}90^\circ$) sequence to generate the solid-echo form of the ^1H NMR transverse relaxation signal $I(t)$. A sequence repetition time of 1 s avoided saturation effects which indicates that the shales are free of inorganic hydrogen with much longer ^1H NMR spin-lattice relaxation times that have been found to occur in Green River oil shales (14).

RESULTS AND ANALYSIS

The peak signal amplitude $I(2\tau)$ normalized per gram of sample at room temperature (which is a measure of the hydrogen concentration contributing to the NMR signal of the specimens) shows a linear correlation with elemental percent hydrogen (w/w) as shown in figure 1 for both the whole and the demineralized shales used in the study. The fact that both the whole and demineralized shales gave the same linearity of $I(2\tau)$ with elemental hydrogen further indicates that the ^1H NMR signals are representative of all the hydrogen in the shales. It is important therefore to know the relative contributions to the ^1H NMR signals of the organic kerogen and the inorganic matrix. Figure 2 compares the temperature variation of the relative ^1H NMR signal amplitudes (normalized per gram of shale) for three shales of different grade with that for a predried montmorillonite sample pyrolysed at 6 K min^{-1} . Analyses of these shales (15) have shown that clays which account for ~ 35% of the inorganic matter are the only significant source of inorganic hydrogen with montmorillonite being the most abundant clay variety. The data in Figure 2 therefore show that the inorganic hydrogen signal is a minor fraction of the total shale signal except for the relatively kerogen-poor ore types such as claystone (ore type III in figure 2). The mineral matter analysis data of Loughnan (15) identified montmorillonite, kaolinite, and illite clays in Rundle shales. From the experimentally determined ^1H NMR signal contributions of montmorillonite and kaolinite and an estimated signal contribution of illite, the calculated signal contributions of the clays in the ore types studied range from ~ 13% for the type III claystone to ~ 6% for the most kerogen-rich type I ore.

A selection of ^1H NMR relaxation signals $I(t)$, recorded at various stages of pyrolysis of a predried shale and its kerogen concentrate are shown in figures 3(a) and 3(b) respectively. These data are typical for all the shales studied. At room temperature the signals for both materials are dominated by a rapidly decaying component, which comprises about 90% of the total signal intensity in the case of

the raw shale. This rapidly decaying component is characteristic of a rigid lattice or "glassy" structure devoid of molecular mobility on a time scale less than $\sim 10^{-5}$ s. The more slowly relaxing minor component of each signal indicates that parts of the structure have a degree of molecular mobility on this time scale, consistent either with extended structural domains being above their glass transition temperature or with a distribution of isolated mobile molecular segments in the structure. As the temperature is raised above room temperature the slower relaxing component increases in intensity at the expense of the rapidly decaying "rigid" signal, suggesting a gradual transition of the structure from the glassy to the mobile state. This occurs earlier and to a greater extent for the demineralized shale. However, even for the shale above ~ 600 K the mobile component accounts for almost all of the signal intensity of the residual specimen. At higher temperatures the total signal intensity falls rapidly as a result of pyrolytic loss of volatile material from the specimen and there is a regrowth of a rapidly decaying signal intensity consistent with the formation of the rigid char residue.

These data were reduced to provide a number of largely independent parameters: (i) The percentage of the total initial signal intensity that is contributed by the rapidly decaying or rigid component (% rigid) is estimated. This estimate is made by fitting an exponential function to the slowly relaxing tail of the signal and extrapolating to the echo peak time of the signal to obtain the mobile signal intensity. The time constant T_2 , of the exponential function is a second parameter which is a measure of the average molecular mobility of the mobile component. These two parameters - % rigid and T_2 - are plotted together against temperature in figures 4a and 4b for a shale and its kerogen concentrate respectively.

(ii) The apparent hydrogen content of the specimen ($\%H$), obtained by calibration of the total 1H NMR signal intensity $I(2\tau)$ for its sensitivity to temperature, is a semi-quantitative parameter useful for monitoring the pyrolytic decomposition and loss of volatile products from the sample. Its temperature dependence for the shale and kerogen concentrate are plotted in figures 5(a) and 5(b) respectively. Also shown in these figures are the differential hydrogen contents computed from these data.

(iii) The analytical second moment M_2^* of the frequency power spectrum representation of the 1H NMR signal (11) which is characteristic of the total signal and enables a qualitative measure of the average molecular mobility of the total specimen to be monitored during the pyrolysis. The temperature variations of M_2^* for the whole and demineralized specimens are also recorded in figures 5(a) and 5(b) respectively.

The apparent hydrogen loss pyrolysis profiles at 4 K min^{-1} for all of the shales were found to be similar. Two outlying profiles of this set are compared in figure 6, and in figure 7 the corresponding M_2^* pyrograms are compared. The temperature of maximum rate of loss of hydrogen as defined by the minimum in the differential percent hydrogen content curve, and the total percentage loss of hydrogen from room temperature to 875 K did not vary significantly (see Table I) between the ore types. This small variation in the total percentage loss for the shale ore types and the linear correlation between this loss when expressed as 1H NMR signal loss normalized per gram of shale and Fischer assay oil yield (figure 8) show that the hydrogen loss during the pyrolysis is predominantly organic.

Previous (16) 1H NMR second moment profiles presented by us on the pyrolysis of Rundle oil shale identified two regions of enhanced molecular mobility of the kerogen during pyrolysis. The first event occurred on heating from room temperature to ~ 500 K and was attributed to a possible glass to rubber transition. This observation is similar to Maddadin and Tawarah's (17) interpretation of an endotherm they detected for a Jordanian oil shale, peaking in the region 433-443 K, as a physical softening and molecular rearrangement of the kerogen, and is also

consistent with Rogers and Cane's (4) description of a "rubberoid" material present after heating to 523 K for a Permian Torbanite. The second less obvious event commenced just prior to onset of the main pyrolysis at ~ 600 K and was attributed to the mobilization of a relatively thermally stable component of the kerogen. These events occurred for all but one of the shales of the present study and in the case of this exception no second softening event was noticeable. Further as illustrated in figure 7 there are considerable variations apparent in details of the ^1H NMR second moment profiles for these ore types which occur above 450 K and which cannot simply be accounted for by differences in the kerogen concentration of the ores. Differences are most apparent above ~ 600 K where there is a wide range of behaviours in the total data for the ore suite as represented in figures 6 and 7 by the extreme examples. These differences certainly do not correlate with kerogen concentration. The temperature at which M_2^* reaches its maximum high temperature value is however, very similar, at ~ 780 K for all ores. For those where the onset of increase in M_2^* is delayed (e.g. ore type I) the rate of increase is greater compared to that of ore types (e.g. ore type XI) where the increase commences earlier.

It can be concluded from these experiments on whole shales that although the behaviour of the different Rundle ore types is similar during heating at the lower temperatures, at higher temperatures and in the zone of main pyrolytic decomposition there are significant differences in the nature of the reacting residues that are particularly evident when the second moment pyrograms are compared. This would suggest the likelihood of corresponding differences in the pyrolysis products of these ore types.

In figures 9 and 10 respectively the sets of ^1H NMR hydrogen loss and M_2^* pyrograms for the demineralized ore types are superimposed for comparison. Clearly there is a close similarity in the pyrolysis behaviour of the kerogens of the various ore types. One conspicuous dissimilarity is at low temperatures where in contrast the raw shales are similar. These low temperature differences are possibly the result of variations in the effect of the demineralization treatment on the different ore types in which some degree of structural degradation occurs however it has not been possible to establish any correlation with the analytical data. The more rapid fall in M_2^* immediately above room temperature for the demineralized as compared to the shale specimens shows lesser inhibition to thermal activation of molecular mobility for the demineralized specimens. This could be contributed to both by covalent bond rupture in the kerogen structure and by reduction of binding interactions at the molecular level between the organic kerogen and the mineral matter. Most of the kerogen structure is transformed from an immobile or rigid lattice state to one of considerable molecular mobility by this low temperature transition during which there is little loss of hydrogen. This low value of M_2^* attained is sustained on further heating until about 650 K while there is only gradual loss of volatile matter to a total loss represented by 15-20% of the hydrogen at 650 K.

The M_2^* pyrograms of all the kerogen concentrates are strikingly similar above 500 K. They all show evidence of the secondary softening event and all the residues undergo a rapid transition from their highly mobile state to a rigid state between 750 K and 770 K. This rapid transition in M_2^* is not reflected in the hydrogen loss programs as a sharp increase but as a sharp decrease in the rate of hydrogen loss at ~ 760 K (figure 10). This is clear evidence of the transition of parts of the mobile material existing in the residue below 750 K by condensation reactions to a rigid state above 770 K. This present evidence for the existence of a transient fluidity in the intermediate kerogen residue complements the microscopic evidence for mesophase formation during the pyrolysis of similar materials by Villey et al (18, 19).

CONCLUSIONS

Notwithstanding the differences in the M_n^* pyrograms at low temperatures these 1H NMR thermal analysis experiments on the demineralized ore types clearly demonstrate the close similarity of all the Rundle oil shale kerogens tested. These Rundle kerogens all exhibit two "softening" events. The first occurs on heating above room temperature and involves the bulk of the structure. The second occurs above 650 K and involves a minor component. There is slow evolution of volatiles between 450 K and 650 K and rapid evolution between 650 K and 750 K. A rapid solidification of the residue occurs between 750 K and 770 K which identifies the secondary softening as a thermoplastic transient event akin to that of bituminous coals.

Given the similarity of the kerogens of all the ore types and the similar mineralogy of the inorganic matrices (15), the differences detected in the pyrolysis behaviour of the ore types must be related to either the concentration differences, or possible variations in the degree of dispersion and/or the nature of the interactions that occur between the organic and inorganic structures. Any of these factors could for example affect the permeability of the shale matrix to evolving molecular species. Thus it can be concluded that the differences observed in shale pyrolysis above 600 K result from differences in the rates of molecular diffusion and losses of mobile pyrolysis products.

ACKNOWLEDGEMENTS

This work was carried out in collaboration with and financially supported by Esso Australia and Southern Pacific Petroleum.

REFERENCES

1. Allred, V.D. Chem. Eng. Progress 62, 55 (1966).
2. Finucane, D., George, J.H. and Harris, H.G. Fuel 56, 65 (1977).
3. Rajeshwar, K. Thermochemica Acta 45, 253 (1981).
4. Rogers, L.J. and Cane, R.F. Aust. Chem. Inst. J. & Proc. 12, 159 (1945).
5. Wen, C.S. and Kobylinski, T.P. Fuel 62, 1269 (1983).
6. Miknis, F.P., Szeverenyi, N.M. and Maciel, G.E. Fuel 61, 341 (1982).
7. Hershkowitz, F., Olmstead, W.N., Rhodes, R.P. and Rose, K.D. In "Geochemistry and Chemistry of Oil Shales", ACS Symposium Series 230 (Eds. F.P. Miknis and J.F. McKay) 301 (1983).
8. Burnham, A.K. and Happe, J.A. Fuel 63, 1353 (1984).
9. Webster, D.S., Cross, L.F. and Lynch, L.J. Rev. Sci. Instrum. 50, 390 (1979).
10. Lynch, L.J. and Webster, D.S. In "Geochemistry and Chemistry of Oil Shales", ACS Symposium Series 230 (Eds. F.P. Miknis and J.F. McKay) 353 (1983).
11. Lynch, L.J., Webster, D.S., Bacon, N.A. and Barton, W.A. In "Magnetic Resonance Introduction, Advanced Topics and Applications to Fossil Energy". (Eds. L. Petrakis and J.P. Fraissard) NATO ASI Series, C 124, 617, Reidel, Dordrecht (1984).
12. Coshell, L. Proc. First Australian Workshop on Oil Shales, Lucas Heights, 25 (1983).
13. Wilson, M.A., Lambert, D.E. and Collin, P.J. Fuel (in press) (1985).
14. Miknis, F.P., Decora, A.W. and Cook, G.L. In "Science and Technology of Oil Shales" (Ed. T.F. Yen) Ann Arbor Science, Ann Arbor, 35 (1976).
15. Loughnan, F.C. "Rundle Oil Shale Mineralogical Analysis of Ore Types", Esso Australia Ltd. Report (1983).
16. Lynch, L.J., Webster, D.S. and Parks, T. Proc. First Australian Workshop on Oil Shales, Lucas Heights, 139 (1983).
17. Haddadin, R.A. and Tawarah, K.M. Fuel 59, 539 (1980).
18. Villey, M., Oberlin, A. and Combaz, A. Carbon 17, 77 (1979).
19. Oberlin, A., Villey, M. and Combaz, A. Carbon 18, 347 (1980).

TABLE I
Analyses and Pyrolysis Data of Rundle Ore Types

Shale Ore Type ¹	F.A. Oil Yield (L/t) Shale	C (%w/w)		Ash (%w/w)		Temperature at Max. Rate of H Loss (K)		Hydrogen Volatile % (298-875K)	
		Shale	Shale	Shale	Demin.	Shale	Demin.	Shale	Demin.
LRC ² I	137	17.50	72.2	16.9	725	725	90	95	
LRC II	134	17.18	71.2	19.5	725	725	93	95	
LRC III	29	6.71	84.0	37.9	725	725	88	91	
LRC IV	63	9.38	83.5	26.7	730	720	87	91	
LRC V	112	15.74	75.2	19.2	725	725	88	92	
LRC ³ VI	56	8.94	82.8	29.8	720	720	91	95	
BK ³ IX	95	14.09	77.1	-	725	725	90	92	
BK XI	56	8.81	82.7	-	720	725	86	92	

¹ Coshell (12)

² Lower Ramsay Crossing seam

³ Brick Kiln seam

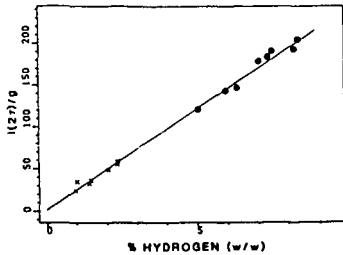


Figure 1. ^1H NMR signal peak intensity ($I(2\tau)$) per gram of specimen versus % elemental hydrogen for Rundle shales (x) and kerogen concentrates (•).

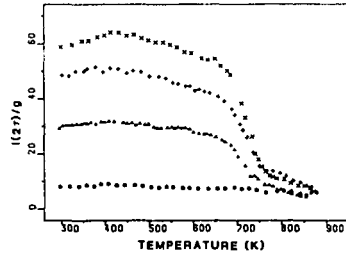


Figure 2. The apparent residual hydrogen per gram of specimen from ^1H NMR measurements versus temperature for Rundle ore types I(x), IX(+), III(Δ) and montmorillonite (•).

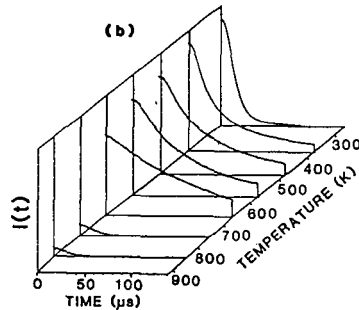
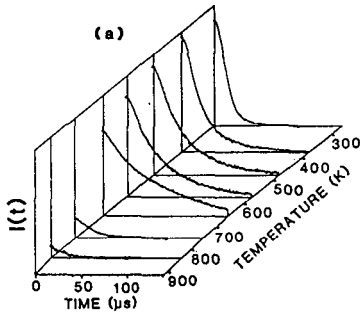


Figure 3. ^1H NMR transverse relaxation signals, $I(t)$, recorded at various temperatures during pyrolysis of (a) the whole shale and (b) the kerogen concentrate of Rundle ore type II.

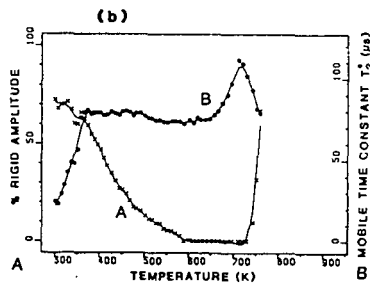
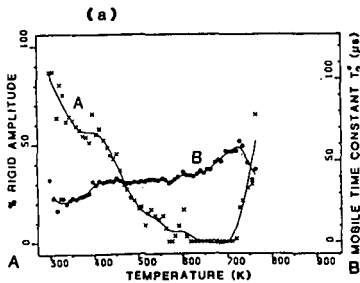


Figure 4. Pyrograms showing the temperature dependences of percentage rigid hydrogen (% Rigid) and the relaxation time constant (T_2) of mobile hydrogen during pyrolysis of (a) the whole shale and (b) the kerogen concentrate for Rundle ore type II.

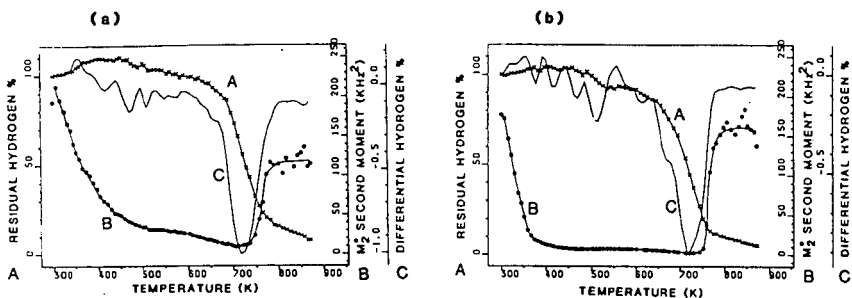


Figure 5. Pyrograms showing the temperature dependences of the apparent residual hydrogen (A), the differential hydrogen content (C) and the ^1H NMR power spectrum second moment, M_2^* , (B) during pyrolysis of (a) the whole shale and (b) the kerogen concentrate of Rundle ore type II.

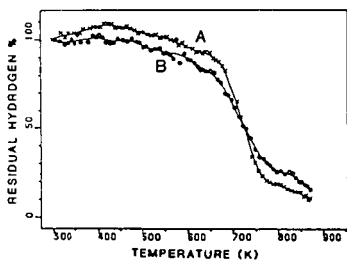


Figure 6. A comparison of pyrograms of the percent apparent hydrogen content for Rundle shale ore types (A) I and (B) XI.

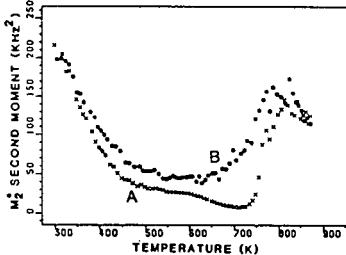


Figure 7. A comparison of the ^1H NMR power spectrum second moment (M_2^*) pyrograms for Rundle shale ore types (A) I and (B) XI.

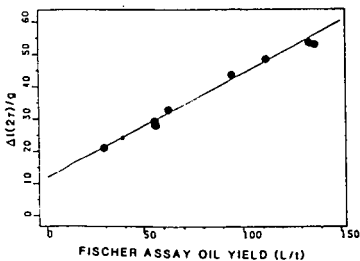


Figure 8. Loss of ^1H NMR signal intensity ($\Delta I(2\tau)$) on heating at 4 K min^{-1} from 298 to 875 K normalized per gram of shale versus Fischer Assay oil yield.

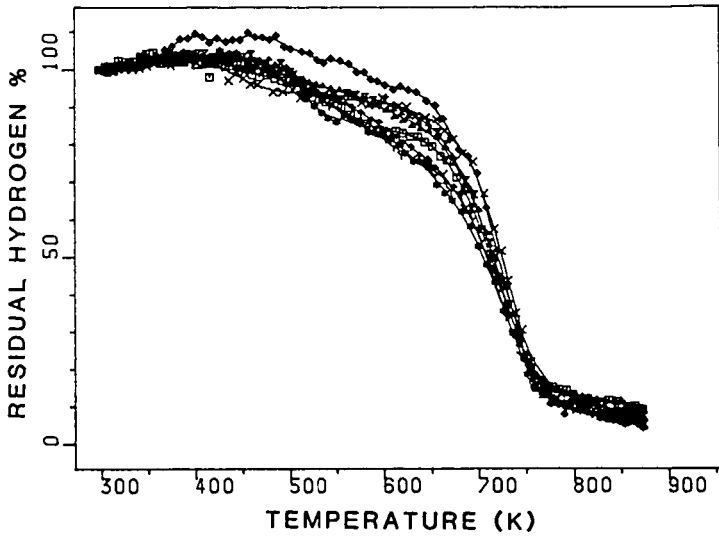


Figure 9. A comparison of pyrograms of the percent apparent residual hydrogen for demineralized specimens of eight Rundle oil shale ore types listed in Table I.

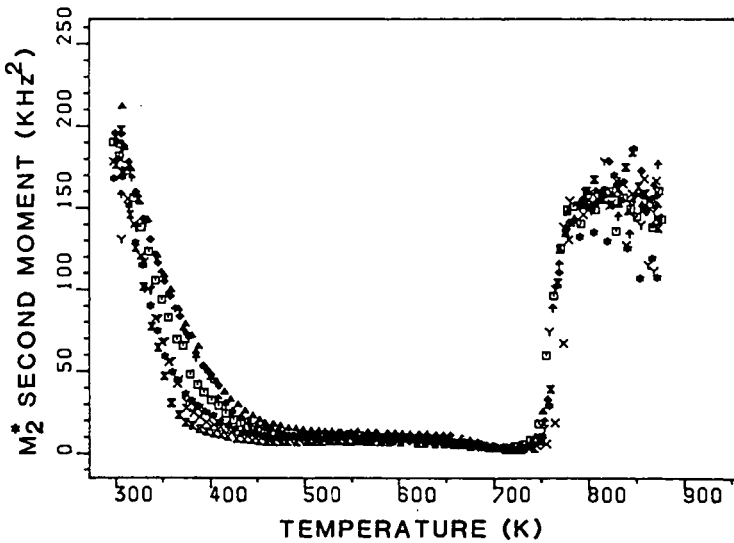


Figure 10. A comparison of the ^1H NMR power spectrum second moment (M_2) pyrograms for kerogen concentrates of eight Rundle oil shale ore types listed in Table I.